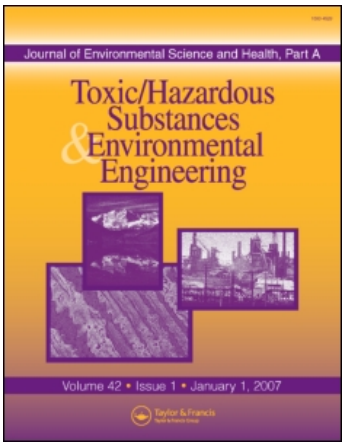

Journal of Environmental Science and Health, Part A
Publication details, including instructions for authors and subscription information:
http://www.informaworld.com/smpp/title~content=t713597268

Quantitative Prediction of Traffic Pollutant Transmission into Buildings

Tsang-Jung Chang [a]; Mei-Yu Huang [a]; Yu-Ting Wu [a]; Chung-Min Liao [a]
[a] Department of Bioenvironmental Systems Engineering, National Taiwan University, Taipei, Taiwan, ROC

Online Publication Date: 01 May 2003

To cite this Article Chang, Tsang-Jung, Huang, Mei-Yu, Wu, Yu-Ting and Liao, Chung-Min(2003)'Quantitative Prediction of Traffic Pollutant Transmission into Buildings',Journal of Environmental Science and Health, Part A,38:6,1025 — 1040

To link to this Article: DOI: 10.1081/ESE-120019861

URL: http://dx.doi.org/10.1081/ESE-120019861

MARCEL DEKKER, INC. • 270 MADISON AVENUE • NEW YORK, NY 10016

JOURNAL OF ENVIRONMENTAL SCIENCE AND HEALTH
Part A—Toxic/Hazardous Substances & Environmental Engineering
Vol. A38, No. 6, pp. 1025–1040, 2003

Quantitative Prediction of Traffic Pollutant Transmission into Buildings

Tsang-Jung Chang,* Mei-Yu Huang, Yu-Ting Wu, and Chung-Min Liao

Department of Bioenvironmental Systems Engineering,
National Taiwan University, Taipei, Taiwan, ROC

ABSTRACT

An integrated air quality model that combines a CFD model and multi-room pollutant transport model has been developed to study the effect of traffic pollution on indoor air quality of a multi-room building located in close proximity to busy roads. The CFD model conducts the large eddy simulation of the three-dimensional turbulent flows and pollutant transport processes in outdoor, whereas the multi-room pollutant transport model performs zonal airflow and pollutant transport in indoor. The integrated model is verified with available field measurement of traffic-induced CO concentrations. Twelve scenarios of numerical experiments for various configurations of window openness are carried out to study the effects of the air change rate and the outdoor pollutant dispersion on indoor air quality. It is concluded that the windward side opening is a significant factor contributing to indoor air quality. Using air inlets on the sideward and leeward envelopes simultaneously can effectively lower the daily mean and peak indoor levels of traffic pollutants and maintain a desirable air change rate.

Key Words: Computational fluid dynamics model; Large eddy simulation; Multi-room pollutant transport model; Indoor air quality; Air pollution control.

*Correspondence: Tsang-Jung Chang, Department of Bioenvironmental Systems Engineering, National Taiwan University, Taipei 10617, Taiwan, ROC; E-mail: tjchang@ccms.ntu.edu.tw.

DOI: 10.1081/ESE-120019861
1093-4529 (Print); 1532-4117 (Online)

MARCEL DEKKER, INC. • 270 MADISON AVENUE • NEW YORK, NY 10016

INTRODUCTION

Natural ventilation has served as an effective design strategy in buildings to secure comfortable indoor environment and to dilute pollutants generated by indoor sources. Clean outdoor air is essential to achieving good performance of natural ventilation. Nevertheless, for some urban areas that traffic pollution is severe, traffic emissions may concentrate at street level and enter indoor environment through open windows or air inlets. As a result, natural ventilation may lead to unacceptable levels of outdoor pollutants for a building located in close proximity to busy roads. To minimize the impact of outdoor traffic pollutants on indoor air quality, numerical modeling regarding the appropriate ventilation control strategy for reducing incoming traffic-induced pollutants and maintaining a desirable air change rate is necessary.

The appropriate ventilation control strategy is determined by the air change rates and the external pollutant dispersion around a building. The air change rate represents the volume it replaces for outdoor air per unit time, and can be regarded as the efficiency of the air mass exchange between indoor and outdoor of a building. The positions of inlet and outlet openings have evident effects on the air change rate so that locating inlet openings at high-pressure surfaces of a building and outlet openings at low-pressure zones can induce significant amounts of air change performance. Nevertheless, for outdoor pollutant levels being high, the indoor pollutant concentration increases as the air change rate increases. When the air change rate approaches to a certain limit, there is no difference between the indoor and outdoor pollutant levels. The external pollutant dispersion around the building is determined by building configurations and pollutant characteristics. For a building located close to busy roads, the windows on the back face of the building have lower levels of traffic pollutants than those on the roadside due to pollutant dispersion. Thus, situating the inlet vent openings on the backsides can noticeably reduce indoor pollutant concentration (Fig. 1). However, these low concentration regions are

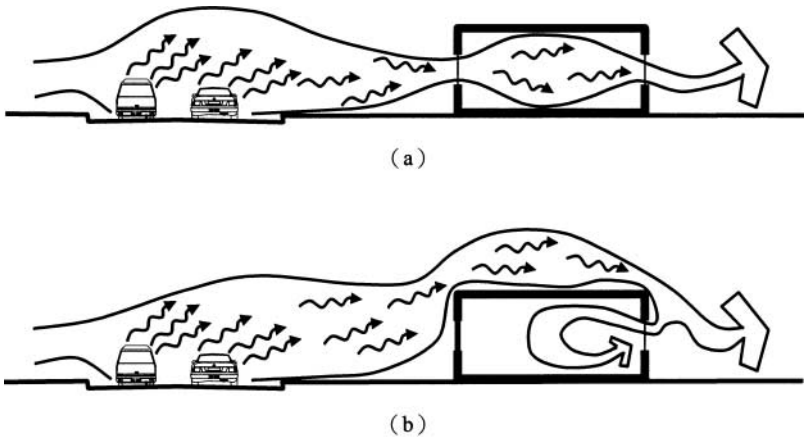

Figure 1. Schematic diagram of the effect of traffic pollution on indoor air quality: (a) windward-sided ventilation; (b) non-windward-sided ventilation.

always at low-pressure surfaces of a building in such that natural ventilation effectiveness cannot be enhanced. To thoughtfully understand the appropriate ventilation control strategy, these two factors should be integratedly considered.

Several researches have developed various air quality models or wind-tunnel experiments to investigate the impact of outdoor traffic pollutants on indoor air quality of a building next to busy roads.[1–9] These works focused on the influence of external flows and canyon flows in pollutant dispersion around single buildings. Some authors have numerically examined wind-driven flow through a single-room building.[10–13] The above researches have only considered either the air change rates or the external pollutant dispersion in a single-room building. Little work on the evaluation of the impact of outdoor traffic pollution on indoor air quality of a multi-room building was reported in the literature, especially the control strategy of ventilation rates and paths for reducing incoming vehicle pollutants and maintaining a desirable air change rate.

Basically there have two different approaches of numerical simulation techniques to study airflow and pollutant transport between indoor and outdoor of buildings, i.e., CFD (Computational Fluid Dynamics) modeling[14] and multi-room pollutant transport modeling.[15,16] Each approach has strengths and limitations. CFD modeling applies a microscopic viewpoint of indoor air quality by using a CFD technique to examine the detailed flow fields and pollutant concentrations within a building, based on the construction of grid meshes for rooms and solving of the coupled energy and Navier–Stokes equations with iterative methods. CFD modeling, allowing detailed numerical simulations of indoor air behavior, indeed provides quantitative information for three-dimensional building conception. However, the grid construction and the solution convergence make CFD models very difficult to implement for a building with more than two rooms. On the other hand, multi-room pollutant transport modeling takes a macroscopic viewpoint of indoor air quality by dividing a building into several rooms connected each other with well-mixing state and evaluating average airflow rates and pollutant concentrations in each room of a building as pollutants are transported through the building and its HVAC system. The air movement and pollutant transport between rooms are calculated as well. But the most difficult problem encountered in the use of this model is the establishment of the pressure coefficients and pollutant concentration coefficients on the building envelope, which are governed by climatic conditions and building geometry. They should be determined by field measurements or numerical simulations. So far only limited information on the pressure coefficients of some regular-shaped buildings is available and there is almost no systematic analysis on the pollutant concentration coefficients.[15,16] For the present study, the study building has five rooms with various geometry and openings in such a way that it is very difficult to use any approach to accurately simulate airflow and pollutant transport between indoor and outdoor. To overcome the limitations of the above two approaches, an integrated air quality model, combining a CFD model and multi-room pollutant transport model, has been developed to investigate the transport of pollutants emitted from motor vehicles through indoor environment. The former conducts the large eddy simulation of the outdoor turbulent flows and pollutant transport processes, whereas the latter performs indoor zonal airflow and pollutant transport.

The main objective of the study is to develop a new integrated air quality model to investigate the transport of pollutants emitted from motor vehicles through indoor environment with multiple rooms. A nonreactive traffic-induced air pollutant, carbon oxide (CO), is used as an indicator of traffic pollution since more than 85% of all the CO in the atmosphere was due to the motor vehicles in many countries.[9] Other pollutants emitted from motor vehicles are not considered herein. Twelve scenarios are performed by setting various configurations of windward, sideward, and leeward window openness. The performance of the air change rate and indoor air quality for each scenario is evaluated. The appropriate control strategy for lowering incoming vehicle pollutants and maintaining a desirable air change rate is suggested.

MODEL DEVELOPMENT AND METHODOLOGY

The integrated air quality model for simulating the transport of CO pollutant emitted from motor vehicles through indoor environment of buildings consists of two parts, namely the computational fluid dynamics model and the multi-room pollutant transport model. The former conducts the large eddy simulation of the turbulent flows and contaminant transport processes in outdoor, whereas the latter performs indoor zonal airflow and pollutant transport.

Computational Fluid Dynamics Model

The three-dimensional CFD model for evaluating the flow field and the dispersion of traffic pollution around buildings includes the airflow field model and the pollutant transport model. The airflow field model is solved first to obtain the velocity and pressure distributions within and around an isolated building. The result of the velocity distribution is next input to the pollutant transport model to calculate the concentration distribution around the building. The airflow around a building is usually considered to be incompressible turbulent flow. The transport of the incompressible turbulent flow is herein simulated by the large eddy simulation (LES). The principle of LES is that the turbulent flow is filtered to remove the small-scale eddies and to leave the large scales of turbulence. The large-scale turbulence is solved explicitly by computing the filtered equations numerically. The influence of the below-filtered scales cannot be neglected and leads to the subgrid stresses (SGS). Let $\bar{u}_i$ and p be the spatially filtered velocity and pressure component in the x_i direction, respectively. The continuity equation and the equations of motion for the filtered velocities with an eddy viscosity representation for the subgrid stresses are

$$\frac{\partial \bar{u}_i}{\partial x_i} = 0 \tag{1}$$

and

$$\frac{\partial \bar{u}_i}{\partial t} + \frac{\partial \bar{u}_i \bar{u}_j}{\partial x_j} = -\frac{1}{\rho}\frac{\partial p}{\partial x_i} + \nu \frac{\partial^2 \bar{u}_i}{\partial x_j \partial x_j} + \frac{\partial}{\partial x_j}\left(\nu_{\text{sgs}} \frac{\partial \bar{u}_i}{\partial x_j}\right) \tag{2}$$

where ρ is fluid density, v is fluid kinematic viscosity, and v_{sgs} denotes the subgrid eddy viscosity. A subgrid model based on an eddy-viscosity closure is used so that v_{sgs} is taken proportional to the numerical grid size and the subgrid energy as follows[12]:

$$v_{sgs} = (Cs\Delta)^2 \left[\frac{1}{2} \left(\frac{\partial \bar{u}_i}{\partial x_j} + \frac{\partial \bar{u}_j}{\partial x_i} \right)^2 \right]^{1/2} \tag{3}$$

in which $\Delta = (\Delta x_i \Delta x_j \Delta x_k)^{1/3}$ is the numerical grid size defined by the geometric average of the finite difference grid space in three directions. C_s is the Smagorinsky constant, for the value used in the present research being 0.16.[12]

The grid-scale mean pollutant concentration C_i within and around an isolated building is predicted by using the filtered pollutant mass conservation equations in the following, which consider convection process, diffusion process, and source emissions, S_i.

$$\frac{\partial C_i}{\partial t} + \frac{\partial \bar{u}_j C_i}{\partial x_j} = \frac{\partial}{\partial x_j} \left((D_{mole} + D_{turb}) \frac{\partial C_i}{\partial x_j} \right) + S_i \tag{4}$$

where D_{mole} and D_{turb} are the molecular and turbulent diffusivity, respectively. The relationship between v_{sgs} and D_{turb} can be linked by the turbulent Schmidt number, which is denoted as $Sc = v_{sgs}/D_{turb}$. In general, the value of the turbulent Schmidt number is between 0 and 1. Herein it is presumed as a constant 0.5, based on the model verification with the wind tunnel experiment.[13] Using the computed mean flow fields described above, the temporal evolution of traffic pollutant around the building is simulated by using Eq. (4).

The above governing equations are numerically solved on a staggered mesh system for the velocity and pressure quantities, which discretized in space using third-order upwind finite differences for the convective terms and second-order central finite differences for others, and in time using the Adams–Bashforth method. The pressure Poisson equation is solved using an iteration method on the staggered mesh. The boundary conditions used in the present research include that, at the inflow boundary, the inflow velocity is in power law profile and remains unchanged with time. No-slip velocity boundary conditions are applied to all solid surfaces and ground. At the outflow and upper boundary, the velocity gradient is set to be zero. Zero gradient condition for the concentration is prescribed to all the boundaries. The initial conditions of both the velocity and concentration fields are set to be zero in the entire computational domain. In addition, the pressure distribution around a building is usually described by dimensionless pressure coefficients.

Multi-room Pollutant Transport Model

The multi-room pollutant transport model, considering wind, thermal buoyancy or a combination of both, can simulate not only typical flow patterns of ventilation in buildings such as crack flow for various window structure, single-sided ventilation, and cross ventilation, but also many flow patterns of HVAC systems. The calculation principle underlying the multi-room model is that buildings are regarded as

complex grid systems of airflow paths, and are composed of joints and connections. Joints represent the zones of the building, whereas the connections between joints simulate airflow paths. The airflow paths include the power-law flow resistance resulting from open or closed doors and windows as well as HVAC systems and can be calculated using the following equation:

$$[D]\{Q^n\} + [K]\left\{\int Q\,dt\right\} = \{F_{\text{wind}}\} + \{F_{\text{temp}}\} + \{F_{\text{HVAC}}\} \tag{5}$$

where Q is the flow rate, n is the power-law exponent of airflow friction, $[D]$ denotes the matrix of airflow friction, $[K]$ is the matrix of room air elasticity, $\{F_{\text{wind}}\}$ represents the power of wind, $\{F_{\text{temp}}\}$ denotes the power of thermal buoyancy, and $\{F_{\text{HVAC}}\}$ is the power of HVAC system.

Besides calculating airflows between zones, the multi-room model also simulates the transport and distribution of pollutants in each room of the building. Simulation of pollutant transport in a multi-room building is based on the assumption that the pollutant concentration is well mixed in a room, and is calculated as follow:

$$[Q]\{C(t)\} + [V]\left\{\frac{dC(t)}{dt}\right\} = \{M(t)\} \tag{6}$$

where $C(t)$ denotes the concentration of a pollutant, $[V]$ is the volume of the rooms, $[Q]$ is matrix of airflow rate obtained in Eq. (5), and $[M]$ is the emission rate of outdoor traffic pollutant.

Prior to the calculation of the multi-room model, the outdoor boundary conditions have to be set up. The outdoor wind velocity, wind direction, and temperature can be obtained by the standard weather data. The pressure coefficient and pollutant concentration at each facade are input from the simulated results of the CFD model. As the aforementioned outdoor boundary conditions are given, the flow rate and pollutant concentration for each joint and connection can be calculated by the solution of a nonlinear system of algebraic equations with the use of the Newton–Raphson iterative method. The flow rate for each joint is next averaged for each room as the average air change rate of the room. Averaging the air change rate of each room for the entire building and divided by the total building volume give the air change rate of the entire building, which represents the volume it replaces for outdoor air per unit time.

MODEL EVALUATION

To secure the confidence and accuracy intervals of the numerical model, an essential element of the numerical model is its evaluation with reliable experimental data. Thus, the present integrated air quality model is verified by a 48-h-period field measurement of outdoor/indoor CO concentrations of a naturally ventilated building given by Green et al.[5] The test building is located close to a busy road with average daily traffic flow of 50,000 vehicles. The outdoor CO concentration was

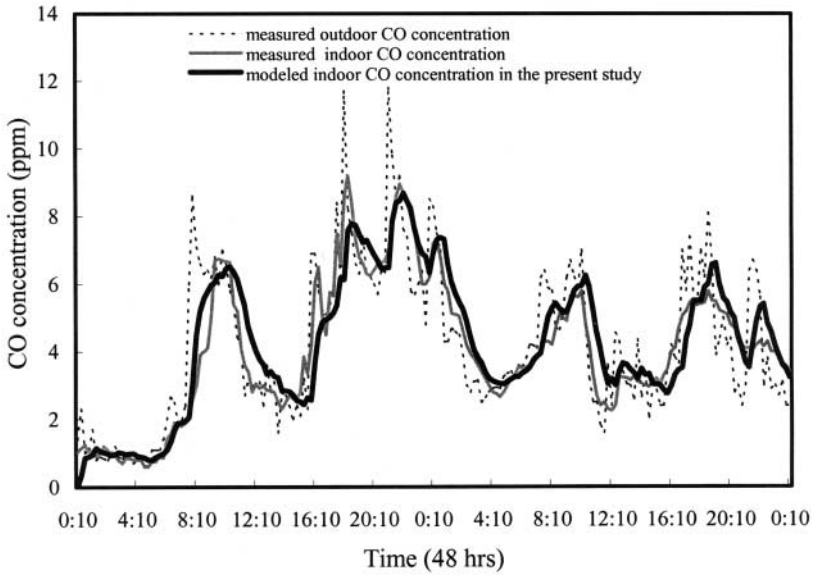

Figure 2. Model evaluation with available measured data.

measured at a window on the roadside facade, whereas the indoor CO concentration was recorded in a room facing the road. There was no internal CO pollutant source in the building. Figure 2 gives the temporal variations of the measured outdoor CO concentration as well as the calculated and measured indoor CO concentration of the test building. It can be seen that the results show good agreement of the concentration distributions between the simulated and measured indoor CO pollutant.

NUMERICAL SCENARIO SIMULATIONS

Under a given outdoor climatic condition and pollutant characteristics, various configurations of windward sideward, and leeward window openness can cause different ventilation rates and paths, resulting in different levels of outdoor-to-indoor airflow and pollutant transport. In Figs. 3 and 4, under an isothermal condition with domain temperature of 25°C, a five-room building with $H = 3.5$ m high, 7.5 m wide, 7.5 m long, and flat roof is considered, which is a common building geometry in USA and Taiwan. Living & dining room and bedroom 1 are in the front part of the building, bathroom in the left, and kitchen and bedroom 2 in the back. Each room of the building has at least one exterior window or door, and the configurations of each exterior window and door are summarized in Table 1. All of the interior doors have the dimension of 0.9 m × 1.8 m and are set to be open. The CO pollutant source is assumed to be a line source continuously emitted from motor vehicles at street level in the entire computational domain, which is located 7.5 m upstream of the building.

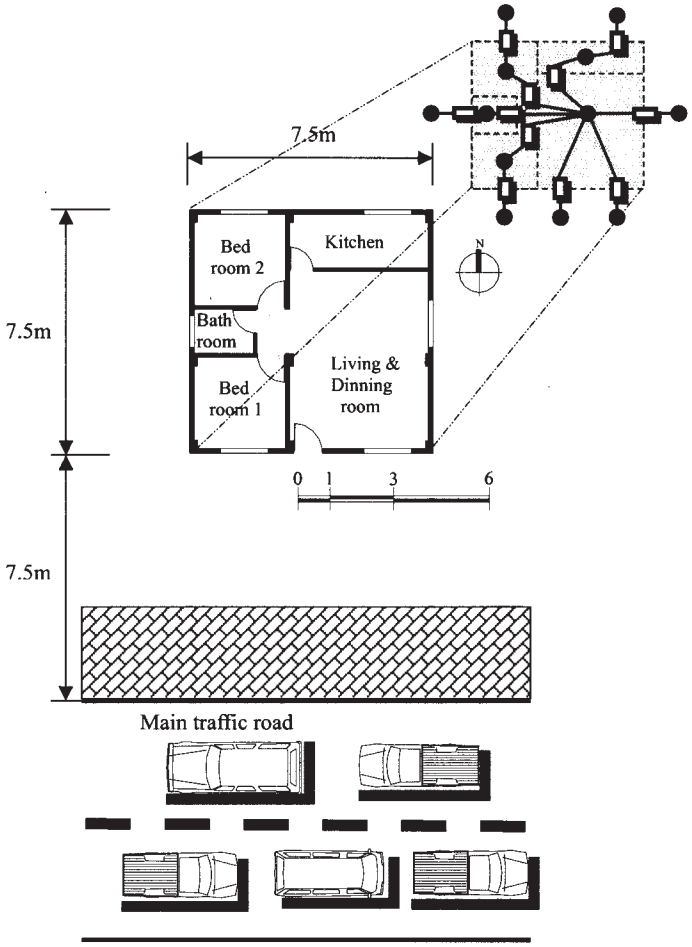

Figure 3. Floor plan of the study building and its representation in a nodal network.

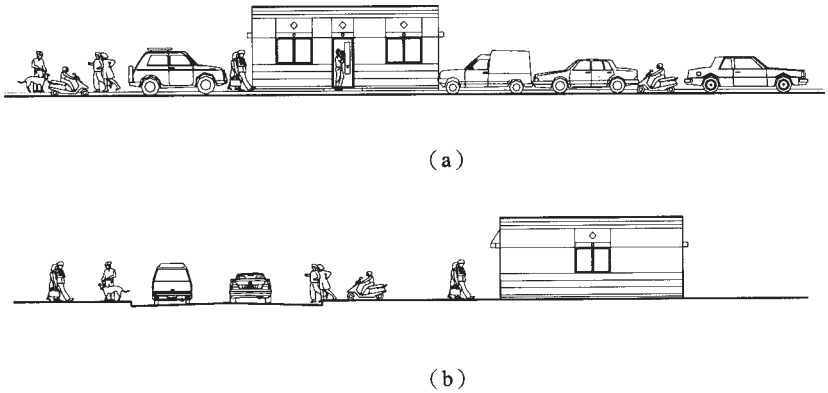

Figure 4. (a) Front; and (b) section view of the study building.

Outdoor Flow: Pressure Coefficient and Pollutant Dispersion Around Building

The computational domain is from $5H$ upstream to $8H$ downstream of the building in the streamwise direction, from $6H$ left hand side to $6H$ right hand side of the building in the lateral direction, and from the ground surface to $8H$ in the vertical direction. A non-uniform grid system with total grid number 18,000 ($30 \times 30 \times 20$) is used. Starting from the building walls, the horizontal grid interval uniformly increases upstream ward, lateral ward, and downstream ward, and increases upward until the upper end. The inflow velocity distribution is power law, $U = U_r(z/z_r)^{0.299}$, where $z_r = 10\,\mathrm{m}$ and U_r is the inflow velocity. U_r is selected to be 0.5 and $2\,\mathrm{m\,s^{-1}}$ since $2\,\mathrm{m\,s^{-1}}$ is a typical average wind speed in Taiwan and $0.5\,\mathrm{m\,s^{-1}}$ is a calm condition for comparison.

The mean airflow velocity fields and the normalized steady-state concentration profiles of $U_r = 2\,\mathrm{m\,s^{-1}}$ at the middle section of the building are illustrated in Figs. 5a and 5b, respectively, for demonstration. The steady-state concentration profiles are normalized by the reference value, C_0, which is the maximum value of pollutant

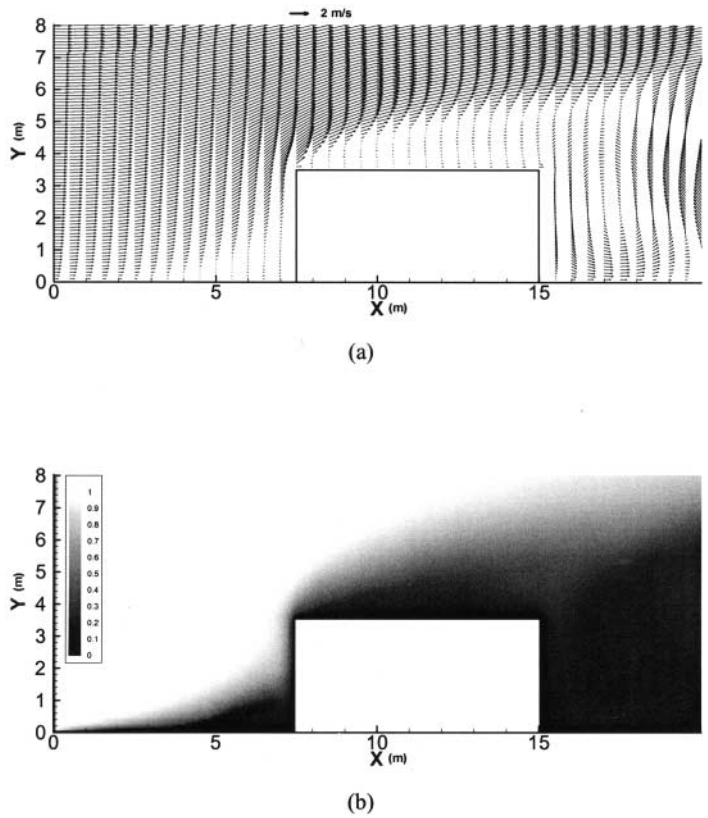

Figure 5. (a) The mean airflow velocity fields; and (b) the normalized CO concentration levels at the middle section of the building ($U_r = 2\,\mathrm{m\,s^{-1}}$).

concentration at the street-level line source. The Reynolds number is about 10^5 based on the height of the building and the free stream velocity. It is observed that there exists a clockwise vortex in front of the building and a large clockwise recirculation zone behind the building is formed. Flow over a building creates a positive pressure zone on the windward side, in which the flow is convection-dominated, and negative zones on the lateral and leeward sides, where the flows are wake-dominated. The calculated pressure distributions around the building are non-dimensionalized as pressure coefficients. Each window and door of the building is given an average value and is summarized in Table 1. Thus, inlet openings situated on the windward wall and outlet openings located on the leeward wall and sidewall can provide good performance of air exchange.

Due to the combined effects of the convection, wake, and turbulent diffusion processes of the velocity field, CO pollutant emitted from a street-level line source follows airflow momentum to approach the building and transport upward over the roof or lateral ward toward the building corners. After passing over the building, pollutants entrain into a large recirculation zone in the back of the building and mix up. The calculated normalized steady-state concentration profiles for each window and door of the building is also given in Table 1 for outdoor wind speeds of 0.5 and $2\,m\,s^{-1}$. From the viewpoint of reducing the impact of traffic pollution, inlet openings on the sideward and leeward sides of the building would be appropriate.

Indoor Flow: Ventilation Control Strategy

Twelve scenarios have been conducted to investigate the effect of traffic pollution on indoor air quality according to various configurations of windward sideward, and leeward window/door openness, which have been summarized in Table 2. The simulated outdoor boundary conditions shown in Table 1 are input into the multi-room pollutant transport model. The air change rate as well as the daily mean and peak indoor concentration of CO pollutant for each room are calculated by using the typical daily CO concentration distribution in Taiwan as depicted in Fig. 6, which shows a two-peak variation during morning and evening rush hours. The building-averaged values of the above calculated results for each scenario are next obtained. The first scenario represents the reference case operating with fully opened windows and doors, resulting in the highest air change rate and the worst levels of traffic pollutant in the building. To thoughtfully understand the relative relationship between each other, the calculated air change rates as well as the daily mean and peak indoor CO levels of the rest of scenarios are compared with the results of the first scenario. Fractional differences in the air change rates and the daily mean indoor CO levels between Scenario 1 and Scenarios 2 to 12 are shown in Fig. 7, whereas the same comparisons except for the daily peak indoor CO levels are depicted in Fig. 8. Consequently, the appropriate ventilation control strategy should have a capability for significantly reducing incoming CO pollutant and maintaining a desirable air change rate. This means that the appropriate ventilation control strategy should be the scenarios having high reduction percentage of the indoor CO level and low reduction percentage of the air change rate, which are situated in the lower right corners of Figs. 7 and 8.

Table 1. Configuration of each exterior window and door on the building envelope.

	Windward envelope			Sideward envelope		Leeward envelope	
	Window 1	Door 1	Window 2	Window 1	Window 2	Window 1	Window 2
Room	Living & dining room	Living & dining room	Bed room 1	Bath room	Living & dining room	Bed room 2	Kitchen
Dimension (m) (width × height)	1.5 × 1.1	1.2 × 1.8	1.5 × 1.1	1.0 × 0.6	1.5 × 1.1	1.5 × 1.1	1.5 × 1.1
Location (m) (lowest height)	1.1	0.05	1.1	1.9	1.1	1.1	1.1
Pressure coefficient	0.70	0.67	0.67	−0.50	−0.45	−0.20	−0.20
Concentration coefficient ($U_r = 0.5\ \mathrm{m\,s^{-1}}$)	1.0	1.0	1.0	0.70	0.70	0.40	0.40
Concentration coefficient ($U_r = 2\ \mathrm{m\,s^{-1}}$)	1.0	1.0	1.0	0.68	0.68	0.37	0.37

Table 2. Twelve scenarios of the numerical simulations.

Scenario	Window openness on windward envelope	Window openness on sideward envelope	Window openness on leeward envelope
1	100%	100%	100%
2	50%	50%	50%
3	1%	1%	1%
4	10%	10%	10%
5	1%	1%	100%
6	1%	100%	1%
7	100%	1%	100%
8	50%	100%	100%
9	1%	100%	100%
10	1%	50%	50%
11	10%	30%	30%
12	1%	30%	100%

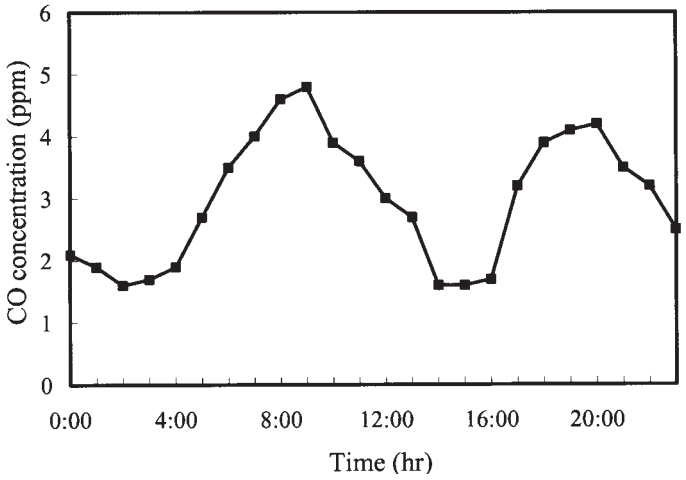

Figure 6. Typical daily CO concentration distribution in Taiwan.

It can be seen from Figs. 7 and 8 that indoor pollutant concentration does not necessarily increase as the air change rate increases. The windward side window/door is a significant factor contributing to the highest air change rates for all scenarios when compared to the non-windward side opening scenarios. As a result of larger amount of polluted air coming into the building, high levels of the daily mean and peak pollutant concentrations within the building can be observed. Scenarios 2, 7, and 8 have acceptable air-exchange performance, however indoor pollutant levels are not effectively reduced. Scenario 3 allows very little outdoor-to-indoor air exchange, resulting in low levels of indoor pollutant concentration. Scenarios 4 and 11 have very low air-exchange performance but together with very high indoor pollutant levels. For the scenarios operating with sideward-sided ventilation

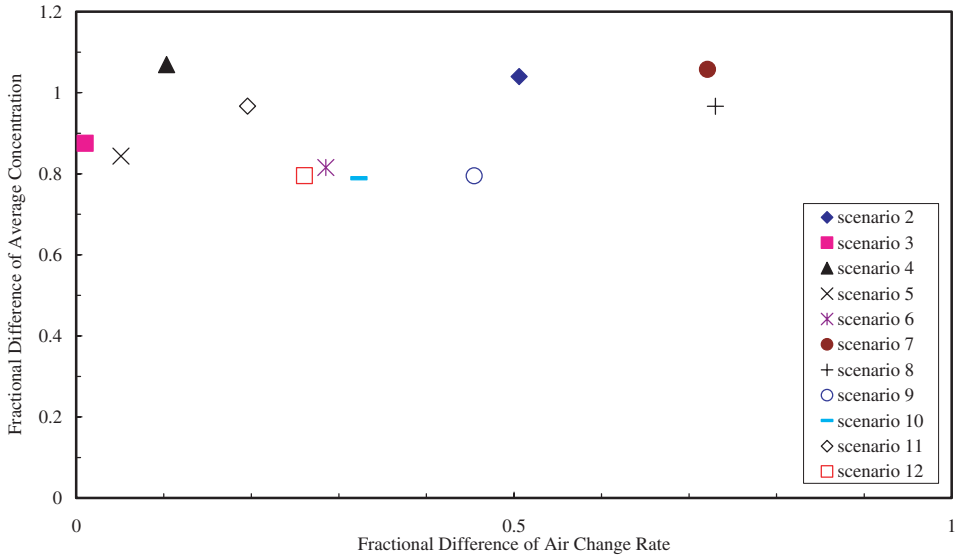

(a)

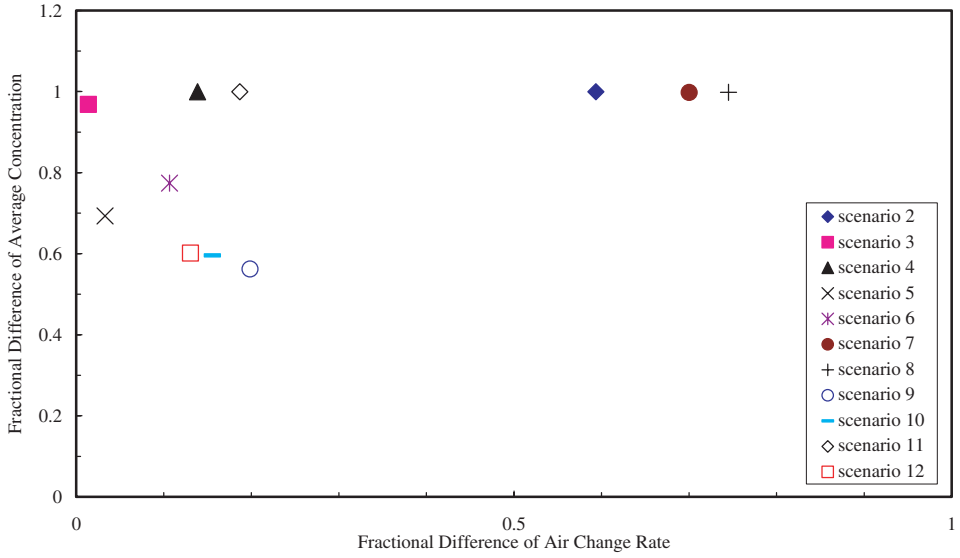

(b)

Figure 7. Fractional differences in the air change rates and the daily mean indoor CO levels between Scenario 1 and Scenarios 2 to 12: (a) $U_r = 0.5\,\mathrm{m\,s^{-1}}$; (b) $U_r = 2\,\mathrm{m\,s^{-1}}$.

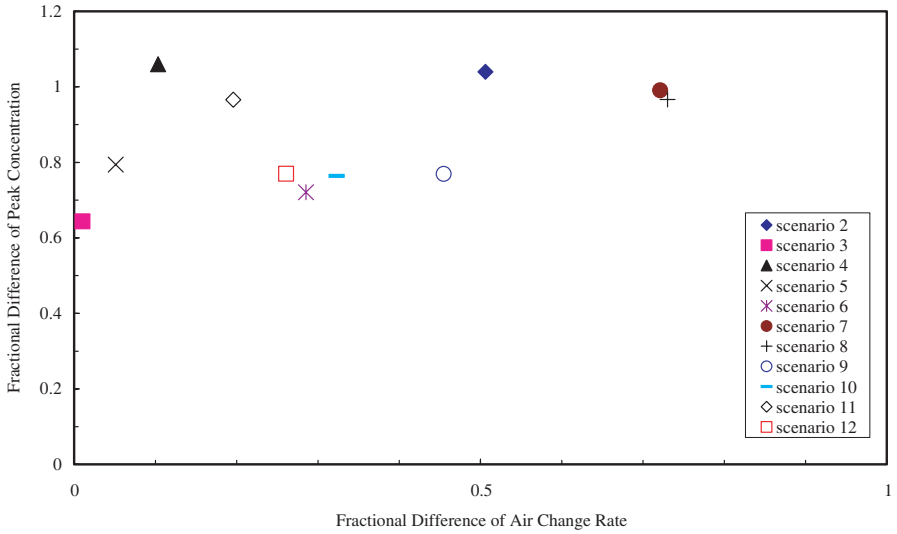

(a)

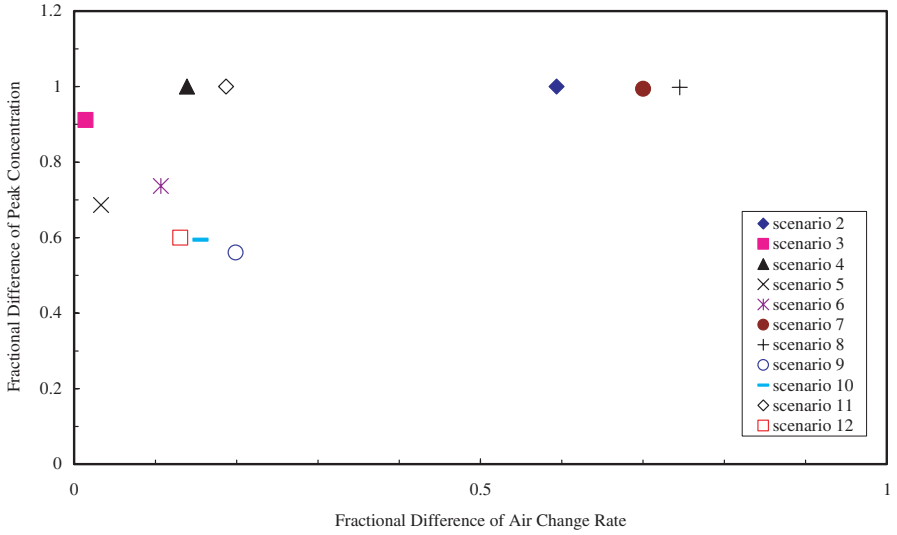

(b)

Figure 8. Fractional differences in the air change rates and the daily peak indoor CO levels between Scenario 1 and Scenarios 2 to 12: (a) $U_r = 0.5\,\mathrm{m\,s^{-1}}$; (b) $U_r = 2\,\mathrm{m\,s^{-1}}$.

only (Scenario 5) or leeward-sided ventilation only (Scenario 6), the reduction of CO pollutant is significant but the corresponding air change rate is relatively low. Scenario 9, using the air inlets on the sideward and leeward envelopes simultaneously, effectively reduces 20–40% of the peak and mean indoor levels of traffic pollutants with maintaining 20–60% of the air change rate and is suggested as the appropriate combined strategy of controlling ventilation rates and paths.

Scenarios 10 and 12 also have good performance because of using the same ventilation strategy as Scenario 9.

CONCLUSIONS

A series of numerical experiments on outdoor-to-indoor airflow and pollutant transport have been successfully conducted to quantitatively investigate the effect of traffic pollution on indoor air quality, based on the newly developed integrated air quality model. This integrated model has a capability for analysis of the appropriate ventilation control strategy for lowering incoming vehicle pollutants and maintaining a desirable air change rate. The present study has led to the conclusion that for all scenarios operating with windward-sided ventilation, the air change rates are high, resulting in high levels of CO pollutant within the building. Scenario 9 uses the air inlets on the sideward and leeward envelopes simultaneously, which is suggested as the appropriate combined strategy for reducing 20–40% of incoming CO pollutant and maintaining 20–60% of the air change rate. It is believed that the present study can contribute an integrated indoor air quality evaluation for naturally ventilated buildings.

ACKNOWLEDGMENT

This work was supported by National Science Council, R.O.C., under grant No. NSC 90-2313-B-002-345.

REFERENCES

1. Mirzai, M.H.; Harvey, J.K.; Jones, C.D. Wind tunnel investigation of dispersion of pollutants due to the wind flow around a small building. Atmospheric Environment **1994**, *28*, 1819–1826.
2. Ekberg, L.E. Relationship between indoor and outdoor contaminants in mechanically ventilated buildings. Indoor Air **1996**, *6*, 41–47.
3. Sini, J.F.; Anquetin, S.; Mestayer, P.G. Pollution dispersion and thermal effects in urban street canyons. Atmospheric Environment **1996**, *30*, 2659–2677.
4. Green, N.E.; Riffat, S.B.; Etheridge, D.W. Ventilation control: effect on indoor concentrations of traffic pollutants. Proceedings of CIBSE A: Building Service Research Technology, **1998**, *19* (3), 149–153.
5. Green, N.E.; Riffat, S.B.; Etheridge, D.W.; Clarke, R. Traffic pollution in and around a naturally ventilated building. Proceedings of CIBSE A: Building Service Research Technology, **1998**, *19* (2), 67–72.
6. Baik, J.J.; King, J.J. A numerical study of flow and pollutant dispersion characteristics in urban street canyons. J. of Applied Meteorology **1999**, *38*, 1576–1589.

7. Huang, H.; Akustu, Y.; Arai, M.; Tamura, M. A two-dimensional air quality model in an urban street canyon: evaluation and sensitivity analysis. Atmospheric Environment **2000**, *34*, 689–698.
8. Chao, Y.H.; Tung, C.W. An empirical model for outdoor contaminant transmission into residential buildings and experimental verification. Atmospheric Environment **2001**, *35*, 1585–1596.
9. Green, N.E.; Etheridge, D.W.; Riffat, S.B. Location of air intakes to avoid contamination of indoor air: a wind tunnel investigation. Building and Environment **2001**, *36*, 1–14.
10. Mistriotis, A.; Bot, G.P.A.; Picuno, P.; Scarascia-Mugnozza, G. Analysis of the efficiency of greenhouse ventilation using computational fluid dynamics. Agricultural and Forest Meteorology **1997**, *85*, 217–228.
11. Ayad, S.S. Computational study of natural ventilation. J. of Wind Engineering and Industrial Aerodynamics **1999**, *82*, 49–68.
12. Jiang, Y.; Chen, Q. Study of natural ventilation in buildings by large eddy simulation. J. of Wind Engineering and Industrial Aerodynamics **2001**, *89*, 1155–1178.
13. Chang, T.J. Numerical evaluation of the effect of traffic pollution on indoor air quality of a naturally ventilated building. J. of Air & Waste Management Association **2002**, *52*, 1043–1053.
14. Awbi, H.B. *Ventilation of Building*; Chapman & Hall: London, UK, 1991.
15. Orme, M. *Applicable Models for Air Infiltration and Ventilation Calculations*; AIVC Technical Note 51, Air Infiltration and Ventilation Center: UK, 1999.
16. Allard, F. *Natural Ventilation in Buildings*; James & James: London, UK, 1998.

Received July 26, 2002